

An evolutionary scenario for the U Scorpii

Ene Ergma¹, Jelena Gerškevič^{1,2} and Marek J. Sarna²

¹ *Physics Department, Tartu University, Ülikooli 18, 50510 Tartu, Estonia*

e-mail: ene@physic.ut.ee; jelen_a@physic.ut.ee

² *N. Copernicus Astronomical Center, Polish Academy of Sciences, ul. Bartycka 18, 00-716 Warsaw, Poland*

e-mail: sarna@camk.edu.pl; jelena@camk.edu.pl

Received; accepted

ABSTRACT

We perform evolutionary calculations of binary stars to find progenitors of systems with parameters similar to the recurrent novae U Sco. We show that a U Sco type–system may be formed starting with an initial binary system which has a low–mass carbon–oxygen white dwarf as an accretor. Since the evolutionary stage of the secondary is not well known, we calculate sequences with hydrogen rich and helium rich secondaries. The evolution of the binary may be divided into several observable stages as: classical nova, supersoft X–ray source with hydrogen stable burning and strong wind phases, ending up with the formation of a massive white dwarf near the Chandrasekhar mass limit. We follow the chemical evolution of the secondary as well as of the matter lost from the system, and we show that observed ¹²C/¹³C and N/C ratios may give some information about the nature of the binary.

Key words: binaries: close — binaries: general — stars: mass loss evolution — stars: recurrent novae — star: individual: U Sco

1 INTRODUCTION

Recurrent novae are a small class of objects which bear many similarities to other cataclysmic variable systems. They experience recurrent outbursts at intervals of 20–80 yrs.

Webbink et al. (1987) lengthily discussed the nature of the recurrent novae, and they concluded that according to outburst mechanisms there are two subclasses of these systems: (a) powered by thermonuclear runaway on the surface of the white dwarf (e.g. U Sco), and (b) powered by the transfer of a burst of matter from the red giant to the main–sequence companion.

U Sco is one of the best observed recurrent novae. Historically, its outbursts were observed in 1863, 1906, 1936, 1979, 1987 and in 1999. Determinations of the system visual luminosity at maximum and minimum, indicate a range $\Delta m_V \sim 9$. We also note that the mean recurrent interval implied by known outbursts is $P_{rec} = 23$ yrs. Schaefer (1990) and Schaefer & Ringwald (1995) observed eclipses of U Sco in the quiescent phase, and determined the orbital period $P_{orb} = 1.23056$ d.

Ejecta abundances have been estimated (from 1979 outburst) from optical and UV studies by Williams et al. (1981) and Barlow et al. (1981). They derived extremely helium rich ejecta $\text{He}/\text{H} \sim 2$ (by number), while the CNO abundance was solar with an enhanced N/C ratio. From the analysis of the 1999 outburst Anupama & Dewangan (2000) obtained

an average helium abundance of $\text{He}/\text{H} \sim 0.4 \pm 0.06$. The estimated mass of the ejected shell for 1979 and 1999 outbursts is $\sim 10^{-7} M_{\odot}$ (Williams et al. 1981; Anupama & Dewangan 2000). Spectroscopically, U Sco shows very high ejection velocities of $(7.5\text{--}11) \times 10^3 \text{ km s}^{-1}$ (Williams et al. 1981; Munari et al. 2000). Latest determinations of the spectral type of the secondary indicate a K2 subgiant (Anupama & Dewangan 2000; Kahabka et al. 1999). Following to Kahabka et al. (1999) the distance to U Sco is about 14 kpc.

According to Kato model (1996), supersoft X–ray emission is predicted to be observed about 10–60 days after the optical outburst. BeppoSAX detected supersoft X–ray emission from U Sco in range 0.2–20 keV just 19–20 days after the peak of its optical outburst in February 1999 (Kahabka et al. 1999). The fact that U Sco was detected as a supersoft X–ray source (SSS) is consistent with steady hydrogen burning on the surface of its white dwarf component.

In this paper we construct several evolutionary sequences which may lead to formation of systems like U Sco. In Section 2 the evolutionary code is briefly described. In Section 3 we discuss the effect of mass transfer on binary evolution. Section 4 contains the results of the calculations. A general discussion and conclusion follow.

2 THE EVOLUTIONARY CODE

The models of secondary stars filling their Roche lobes were computed using a standard stellar evolution code based on the Henyey–type code of Paczyński (1970), which has been adapted to low–mass stars (Marks & Sarna 1998, hereafter MS98).

Our nuclear reaction network is based on that of Kudryashov & Ergma (1980), who included the reactions of the CNO tri–cycle in their calculations of hydrogen and helium burning in the envelope of an accreting neutron star. We have included the reactions of the proton–proton (PP) chain. Hence we are able to follow the evolution of the elements: ^1H , ^3He , ^4He , ^7Be , ^{12}C , ^{13}C , ^{13}N , ^{14}N , ^{15}N , ^{14}O , ^{15}O , ^{16}O , ^{17}O and ^{17}F . We assume that the abundances of ^{18}O and ^{20}Ne stay constant throughout the evolution. We use the reaction rates of: Fowler, Caughlan & Zimmerman (1967, 1975), Harris et al. (1983), Caughlan et al. (1985), Caughlan & Fowler (1988), Bahcall & Ulrich (1988), Bahcall & Pinsonneault (1992), Bahcall, Pinsonneault & Wesserburg (1995) and Pols et al. (1995). We use the Eggleton (1983) formula to calculate the size of the secondary’s Roche lobe.

For radiative transport, we use the opacity tables of Iglesias & Rogers (1996). Where they are incomplete, we fill the gaps using opacity tables of Huebner et al. (1977). For temperatures lower than 6000 K we use the opacities given by Alexander & Ferguson (1994) and Alexander (private communication). For a more detailed description of the code see MS98.

3 THE EFFECTS OF MASS TRANSFER

While calculating evolutionary models of binary stars, we must take into account mass transfer and associated physical mechanisms which lead to mass and angular momentum loss. Apart from angular momentum loss due to gravitational wave radiation and magnetic braking, there is additional loss due to the non–conservative nature of semidetached evolution, such as novae outbursts and strong optically thin/thick wind from white dwarf occurring during stable hydrogen shell burning phase.

We can express the change in the total orbital angular momentum (J) of a binary system as

$$\frac{\dot{J}}{J} = \frac{\dot{J}}{J}\Big|_{\text{GWR}} + \frac{\dot{J}}{J}\Big|_{\text{MSW}} + \frac{\dot{J}}{J}\Big|_{\text{NOAML}} + \frac{\dot{J}}{J}\Big|_{\text{FAML}} + \frac{\dot{J}}{J}\Big|_{\text{FWIND}} \quad (1)$$

where the terms on the right hand side are due to: gravitational wave radiation, magnetic stellar wind braking, novae outbursts angular momentum loss (which describe the loss of angular momentum from the system due to non–conservative evolution), frictional angular momentum loss (which occurs during a novae outburst as the secondary orbits within the expanding novae shell and during strong optically thin/thick wind) and optically thin/thick wind from white dwarf (during stable hydrogen shell burning). The role of the first two terms have been discussed in many papers (see, for example, review paper by Verbunt 1993). In our paper we discuss the last three terms.

3.0.1 Angular momentum loss associated with novae outbursts

To take account of the angular momentum loss that accompanies mass loss due to novae outbursts that occur on the surface of the white dwarf during the semidetached phase, we use a formula based on that used to calculate angular momentum loss via a stellar wind (Paczynski (1967); Ziółkowski (1985) and De Greve (1993)),

$$\frac{\dot{J}}{J}\Big|_{\text{NOAML}} = f_1 f_2 \frac{M_{wd} \dot{M}_{sg}}{M_{sg} M_{tot}}, \quad \text{where } \dot{M} = f_1 \dot{M}_{sg}. \quad (2)$$

f_1 is the ratio of the mass ejected by the white dwarf to that accreted by the white dwarf; f_2 is defined as the effectiveness of angular momentum loss during mass transfer (Sarna & De Greve 1994, 1996); M_{wd} and M_{sg} denote mass of white dwarf primary and subgiant secondary, respectively; M_{tot} ($=M_{wd} + M_{sg}$) is the total mass of the system; \dot{M} and \dot{M}_{sg} are, respectively, the rate of mass loss from the system and the rate of mass loss from the secondary ($-\dot{M}_{sg}$ is equivalent to the mass transfer rate). We take $f_2 = 1.0$ which is typical for a stellar wind. Recently, Livio & Pringle (1998) proposed a model in which the accreted angular momentum is removed from the system during novae outbursts, which agrees with our earlier suggestions (Marks, Sarna & Prialnik 1997, MS98). Equation (2) is in quantitative agreement with estimations made by Livio & Pringle (1998).

3.1 Frictional angular momentum loss

During nova outburst or optically thin/thick wind phase the secondary star effectively orbits within the expanding nova shell or dense wind matter. Due to the frictional deposition of orbital energy into expanding nova shell or strong wind, the separation of the components will be decreased.

Livio, Govarie & Ritter (1991) estimated the change in the orbital angular momentum brought about by frictional angular momentum loss over a complete novae cycle,

$$\frac{\dot{J}}{J}\Big|_{\text{FAML}} = \frac{1}{4} (1 + q) \frac{(1 + U^2)^{\frac{1}{2}}}{U} \left(\frac{R_{sg}}{a}\right)^2 \frac{\dot{M}_{wind}}{M_{sg}}, \quad (3)$$

where U is the ratio of the expansion velocity of the envelope at the position of the secondary to the orbital velocity of the secondary in the primary’s frame of reference ($v_{\text{exp}}/v_{\text{orb}}$), ($q = M_{wd}/M_{sg}$) is the mass ratio and \dot{M}_{wind} is the rate of mass flow past the secondary Warner (1995). For strong winds from white dwarf during stable hydrogen shell burning Hachisu, Kato & Nomoto (1996) estimated $v_{\text{exp}}/v_{\text{orb}} \sim 10$. Since we have no information concerning the expansion velocity of the ejecta from theoretical novae models of Prialnik & Kovetz (1995) and Kovetz & Prialnik (1997) (hereafter PK95 and KP97), we do not include the effect of frictional angular momentum loss during nova phase. We include this effect during strong wind phase.

3.2 Optically thin/thick wind angular momentum loss

If we consider a carbon–oxygen (C–O) white dwarf accreting matter from a companion with solar composition, there exists a critical accretion rate above which the excess material

is blown off by strong wind. Hachisu et al. (1996) show that because wind velocity is about 10 times higher than orbital velocity, the wind has the same specific angular momentum as that of the white dwarf, which is estimated as

$$\left. \frac{\dot{J}}{J} \right|_{\text{FWIND}} = \frac{q}{1+q} \frac{\dot{M}_{wind}}{M_{sg}}. \quad (4)$$

As argued by MS98, for typical binary parameters, angular momentum loss due to nova outbursts and magnetic stellar wind braking are the dominant angular momentum loss mechanisms, with gravitational wave radiation two orders of magnitude less effective (when the orbital period decreases sufficiently, gravitational wave radiation will be more effective). Frictional angular momentum loss is the least effective at eight orders of magnitude less than novae outbursts angular momentum loss and magnetic stellar wind braking. However this mechanism will be very effective during strong optically thin/thick wind (SSS phase). Note also, that during the wind phase the wind carries off the specific angular momentum of the white dwarf, which stabilizes the mass transfer (Hachisu et al. 1996; Li & van den Heuvel 1997).

3.3 Accretion of material ejected during novae outbursts

We employ the code developed by MS98, which utilises the results of the theoretical novae calculations made by PK95 and KP97. By interpolation from the data sets of PK95 and KP97, at each time-step, we use the white dwarf mass and the mass transfer rate to determine the novae characteristics: f_1 , amplitude of the outburst, recurrence period, chemical composition of the ejected material.

To calculate the re-accretion by the secondary of material ejected during novae outbursts, we assume that the mass of the material re-accreted (M_{re-acc}) is proportional to the mass of the material ejected by the white dwarf such that,

$$M_{re-acc} = \left(\frac{R_{sg}^2}{4a^2} \right) M_{ej}, \quad (5)$$

where M_{ej} is the amount of matter ejected in the nova outburst, R_{sg} and a are the radius of the secondary star and the separation of the system, respectively. The constant of proportionality is the ratio of the cross-sectional area of the secondary star to the area of a sphere at radius a from the white dwarf. We base this formula on the assumption that novae ejections are spherically symmetric and instantaneous.

3.4 Accretion of material from strong wind

We define two critical mass accretion rate onto white dwarf. First (Warner 1995):

$$\dot{M}_{cr,1} = 2.3 \times (M_{wd} - 0.19)^{3/2}, \quad (6)$$

describing critical accretion rate above which hydrogen rich material is burning in a stable shell; and below which novae outbursts occur. Second (Nomoto, Nariai & Sugimoto 1979; Hachisu et al. 1996):

$$\dot{M}_{cr,2} = 9.0 \times (M_{wd} - 0.5), \quad (7)$$

describing the critical accretion rate above which strong wind solution by Hachisu et al. (1996) is working. It allows burning of the hydrogen into helium at a rate close to $\dot{M}_{cr,2}$, with the excess material being blown off by the wind at the rate:

$$\dot{M}_{wind} = \dot{M}_{sg} - \dot{M}_{cr,2}. \quad (8)$$

To calculate re-accretion of material from the wind by the secondary, we assume that, similarly to eq. 5, the mass of re-accreted material is proportional to the mass of material loss by the white dwarf due to strong wind (\dot{M}_{wind}).

4 RESULTS OF CALCULATIONS

Since the evolutionary stage of the secondary (hydrogen or helium rich) is not observationally determined (more details in section 5), we computed four different sequences with hydrogen and helium rich secondaries. Initial parameters of the sequences are presented in Table 1.

Table 1 Initial parameters of computed sequences

model	M_{sg} [M_{\odot}]	M_{wd} [M_{\odot}]	P_i (RLOF) [d]	X	Z
A	1.4	0.70	1.34	0.7	0.02
B	1.7	0.85	1.61	0.7	0.02
C	1.4	0.70	1.26	0.5	0.02
D	1.7	0.85	1.24	0.5	0.02

The sequences C and D present a helium rich SSS channel proposed by Hachisu et al. (1999). In Table 2 we present results for computed sequences. The orbital parameters are given at the moment when orbital period is equal to 1.23 d. The effective temperature and luminosity are for subgiant star.

According to our calculations, all models go through the short time first nova phase (n1). We have used the grid of models calculated by PK95, KP97 and their classification scheme to relate theoretical models to observations of nova outburst (for more details see MS98). After that, systems enter into the first stable hydrogen burning phase (s1), which is followed by the wind phase (w). The sequences B, C and D have wind phase and second stable hydrogen burning phase (s2). The sequence A does not exhibit wind phase, and after stable burning phase this system evolves into second nova phase (n2). After second stable hydrogen burning phase sequences B and C evolve through recurrent novae phase. In Table 3 we give the duration of each phase. The duration of the SSS stage (stable hydrogen burning and wind phases) is ranging from several hundred thousand to several million years. During the second nova phase, sequence A shows behaviour characteristic for slow novae. Sequence D avoids second novae phase, and for this system the white dwarf mass will exceed Chandrasekhar limit during stable hydrogen burning, and a supernova explosion may occur.

U Sco progenitors can be found with the help of evolutionary sequences B (hydrogen rich) and C (helium rich). After stable hydrogen burning stage both sequences enter into recurrent nova phase (Fig.1). In Fig. 2 the evolution of the mass accretion rate versus orbital period is shown for two sequences B and C. From Fig. 2 we see that both systems evolve through the orbital period $P_{orb} = 1.23$ d twice.

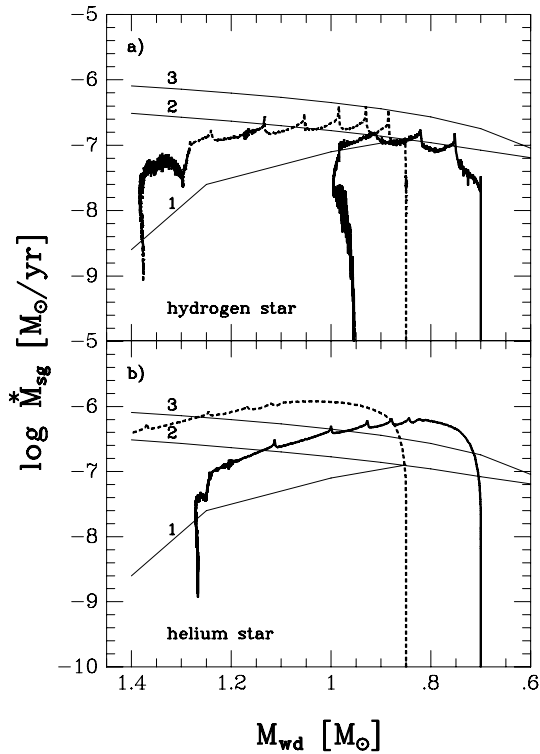


Figure 1. The evolution of the mass transfer rate versus white dwarf mass: (a) for hydrogen rich star as donor (sequences A, B in Table 1), and (b) for helium rich star as donor (sequences C, D in Table 1). The stable hydrogen burning and wind solutions are shown. The lines marked 1, 2 and 3 shows lower boundaries for recurrent novae, stable hydrogen burning and strong wind regions, respectively. The region restricted by lines 1 and 2 shows the recurrent nova phase.

Table 2 Results for computed sequences

model	M_{sg} [M_{\odot}]	M_{wd} [M_{\odot}]	$\log T_{\text{eff}}$ [K]	$\log L/L_{\odot}$	\dot{M}_{sg} [$M_{\odot} \text{ yr}^{-1}$]
A	0.545	0.983	3.669	0.153	2.02×10^{-8}
B	0.936	1.304	3.693	0.416	3.58×10^{-8}
C	0.603	1.255	3.721	0.388	4.09×10^{-8}
D	1.696	0.852	3.957	1.707	1.14×10^{-8}

During the first crossing of $P_{orb} = 1.23d$ line the luminosity of the secondary is too high ($\log L/L_{\odot} \sim 0.9$ and 1.35 for sequences B and C, respectively) and it does not fit the observed absolute magnitude $M_V = +3.8$ of U Sco.

For the same two evolutionary sequences, in Fig. 3 we present evolution of the orbital period P_{orb} versus mass of subgiant M_{sg} (Fig. 3a) and mass of the white dwarf M_{wd} (Fig. 3b). From grid of models (PK95 and KP97) we find $A=7.6$ mag, and $P_{rec}=23$ and 54 yrs for sequences B and C, respectively. Therefore, we can conclude that sequence B gives the best fit to observing parameters of U Sco.

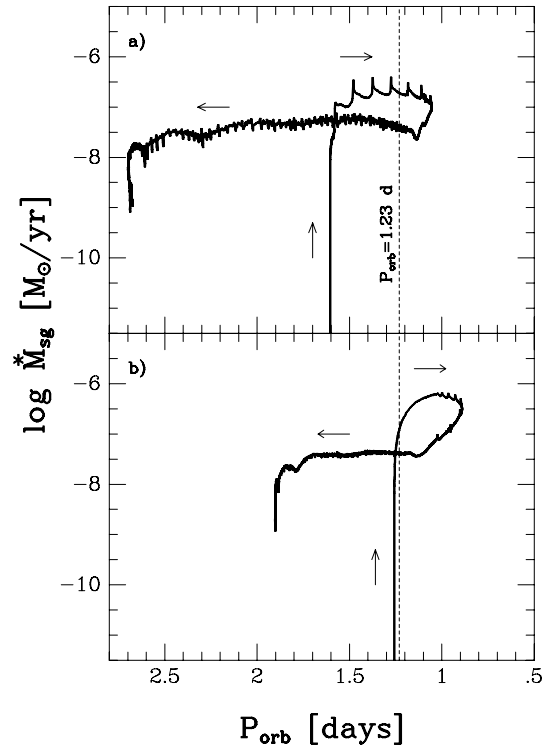


Figure 2. The evolution of the mass transfer rate versus the orbital period of the system: (a) for hydrogen rich star as donor (sequence B in Table 1, 2), and (b) for helium rich star as donor (sequence C in Table 1, 2). The arrows show the directions of evolution. The vertical (thin dashed) line marks the position of the U Sco orbital period.

Table 3 Time-scales for evolutionary phases

model	$\Delta t_{\text{novae}}^1$	Δt_{stat}^1	Δt_{wind}	Δt_{stat}^2	$\Delta t_{\text{novae}}^2$
			[$\log(\Delta t/\text{yr})$]		
A	4.00	6.57	–	–	8.17
B	5.97	5.53	3.70	6.40	7.05
C	4.76	5.41	5.39	6.17	7.30
D	4.89	5.02	5.60	5.58	–

4.1 Chemical composition of the subgiant and ejected matter

Our program is able to follow in detail the evolution of the chemical composition of the subgiant and the ejected matter. In Table 4 we show isotopic composition in the envelope of the subgiant and the ejected matter for two sequences B and C, for a moment when the binary system has orbital period $P_{orb}=1.23$ d.

If we compare the helium rich model C with the hydrogen rich model B we can see that N/C ratio in the envelope of the subgiant is higher for helium rich model than hydrogen rich one, but the isotopic ratio $^{12}\text{C}/^{13}\text{C}$ is higher for the hydrogen rich model. In the ejected matter both ratios are similar.

Our theoretical calculations show that He/H ratio for the matter lost from the system changes during evolution from 0.56 to 1.26. For evolutionary sequences B and C and

Table 4 Chemical compositions for sequence B and C

model	^{12}C [$\times 10^{-3}$]	^{13}C [$\times 10^{-4}$]	^{14}N [$\times 10^{-3}$]	^{15}N [$\times 10^{-7}$]	^{16}O [$\times 10^{-3}$]	^{17}O [$\times 10^{-5}$]	$^{12}\text{C}/^{13}\text{C}$	N/C
B subgiant	1.41	3.05	3.16	5.64	9.77	0.58	4.6	1.8
B ejecta	2.81	11.51	42.06	251.60	1.77	200.00	2.4	10.6
C subgiant	0.41	1.40	4.53	2.71	9.79	1.17	2.9	8.2
C ejecta	1.94	6.97	37.10	83.78	4.94	68.48	2.8	14.0

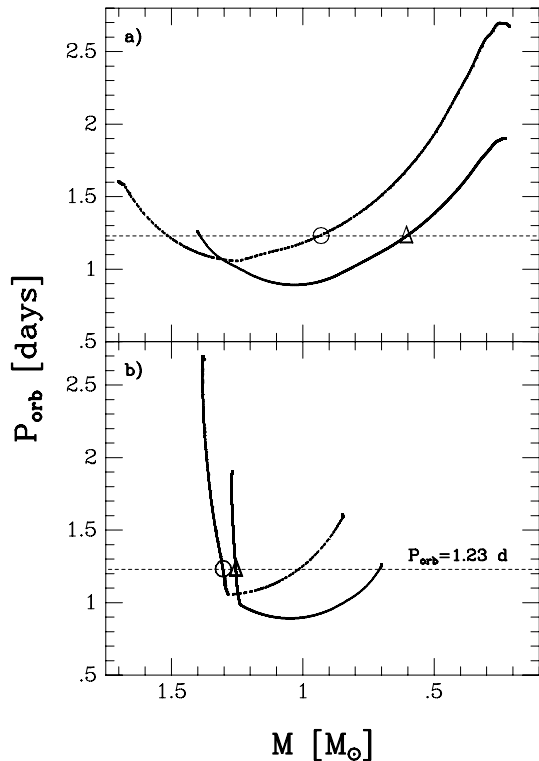


Figure 3. The evolution of the orbital period of the system as a function (a) of the subgiant mass M_{sg} : solid line – sequence C, dashed line – sequence B, and (b) of the white dwarf mass M_{wd} : solid line – sequence C, dashed line – sequence B. Horizontal thin dashed lines mark orbital period for U Sco, open circle mark positions of subgiant and white dwarf masses for sequence B, open triangle for sequence C. For upper panel evolution is going from left to right, for lower panel from right to left.

for the orbital period of U Sco, this ratio is about 0.7. Our He/H determination is well inside observational determination which vary between 0.4 and 2 (Anupama & Dewangan 2000, Williams et al. 1981).

Figs. 4 and 5 show the evolution of the abundances of helium, hydrogen, carbon, nitrogen and oxygen of the subgiant envelope and ejected matter. The vertical thin dashed lines show the place where the orbital period is equal to 1.23 d. In Fig.5 we also identify the phases of the binary system evolution: n1 – first short time nova episode, s1 – first stable hydrogen burning phase, w – strong wind phase, s2 – second stable hydrogen burning phase and n2 – second nova phase.

Chemical composition and isotopic analysis may give more information about the evolutionary stage of U Sco. Possible observational tests are discussed in detail by MS98.

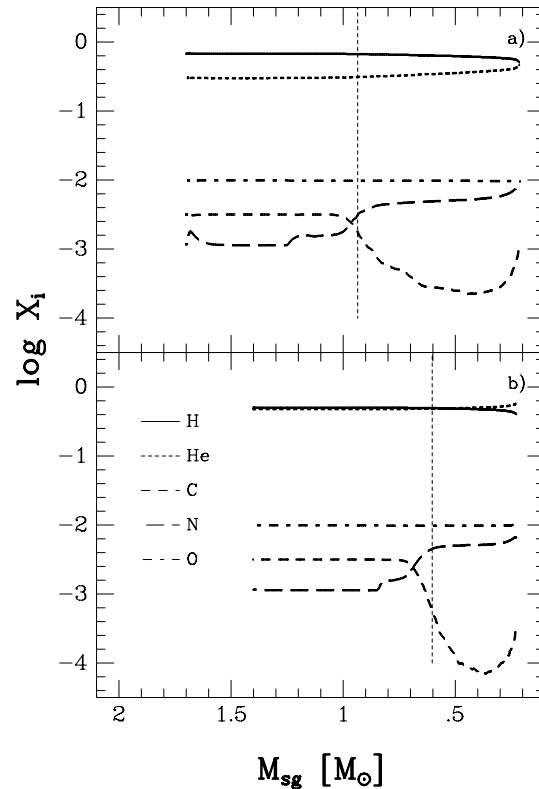


Figure 4. The evolution of the red giant surface abundances of H, He, C, N and O as a function of the subgiant mass M_{sg} : upper panel – sequence B, lower panel – sequence C. Vertical thin dashed lines mark the position of subgiant mass for sequences B ($M_{sg} = 0.926 M_{\odot}$) and C ($M_{sg} = 0.603 M_{\odot}$) respectively (see Table 2 for more details).

Unfortunately, the subgiant component in U Sco is too faint for infrared spectroscopic observations of CO bands in order to determine the $^{12}\text{C}/^{13}\text{C}$ ratio. However, we think that blue domain spectra of U Sco could show some absorption structure in the region of 4216\AA in the CN sequence like one observed for DQ Her (Chanan, Nelson & Margon 1978, Schneider & Greenstein 1979, Willimas 1983). Analysis of this region of the spectra is more complicated because the structure of the CH and CN violet system can be affected by some absorption features from the disc. However, we suggest that since the matter in the accretion disc reflects the chemical composition of the subgiant star, analysis of the disc will give us the information we need if we use observations made during the quiescent phase. The chemical analysis of the expanding envelope (Anupama & Dewangan 2000) also

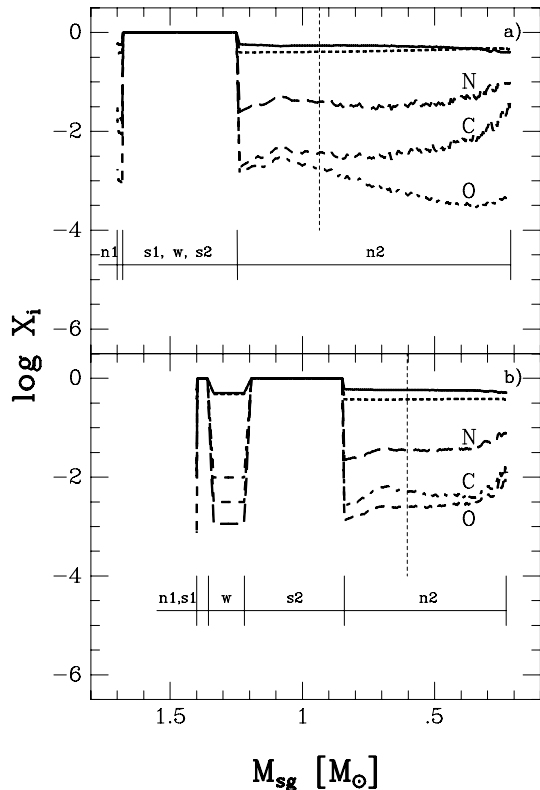


Figure 5. The evolution of the ejected matter abundances of H, He, C, N and O as a function of the subgiant mass M_{sg} : upper panel – sequence B, lower panel – sequence C. For more explanation see text.

will give useful information allowing comparison with theoretical models (see Table 4).

5 DISCUSSION

Hachisu et al. (1999) proposed a new evolutionary path to SNe Ia, in which the companion star is helium-rich. In their model, typical orbital parameters of SNe Ia progenitors are: $M_{wd} = 1.37 M_{\odot}$, $M_{sg} \sim 1.3 M_{\odot}$, and $\dot{M}_{sg} \sim 2 \times 10^{-7} M_{\odot} \text{ yr}^{-1}$. Based on light-curve analysis, Hachisu et al. (2000) also constructed a detailed theoretical model for U Sco. They found that the best fit parameters are: $M_{wd} \sim 1.37 M_{\odot}$, and $M_{sg} \sim 1.5 M_{\odot}$ (a range from 0.8 to 2.0 M_{\odot} is acceptable).

However, the helium enriched model poses a serious problem. Truran et al. (1988) discussed the composition dependence of thermonuclear runaway models for the recurrent novae of U Sco-type. They showed that for $M_{wd} = 1.38 M_{\odot}$, $\dot{M}_{sg} = 1.5 \times 10^{-8} M_{\odot} \text{ yr}^{-1}$, $L = 0.1 L_{\odot}$ optically bright outbursts are obtained only for matter with $\text{He}/\text{H} < 1-2$. Above results are consistent with our sequences B and C where He/H are equal 0.48 and 0.96, respectively.

There is an alternative explanation of helium enrichment as observed in U Sco which may also occur due to helium enriched winds from the white dwarf (Priyalnik & Livio 1995).

According to Kato (1996), the supersoft component in

UV spectrum is predicted to be observable about 10 days after the outburst. For hydrogen-rich model ($\text{He}/\text{H} = 0.1$) the supersoft X-ray component is expected to rise till ~ 50 days after the outburst to a maximum luminosity of $\sim 3 \times 10^{36} \text{ ergs}^{-1} (d/kpc)^2$. For helium-rich model ($\text{He}/\text{H} = 2$), the maximum luminosity is reached about 20 days after the optical outburst. Unfortunately, Kahabka et al. (1999) could follow the X-ray outburst of U Sco for only 19–20 days after outburst. According to Kato (1996), the X-ray luminosity behaviour depends on the chemical composition. Therefore, the evolution of the X-ray luminosity may give the important evidence about the chemical composition of the accreted matter.

6 CONCLUSION

We calculated several evolutionary sequences to reproduce orbital and physical parameters of the recurrent novae of U Sco-type. We showed that U Sco systems possibly form from binaries with a low-mass C–O white dwarf as accretor. Such a system evolves through several observable stages: recurrent nova, SSS with stable hydrogen burning and SSS with strong wind phases. In final phase of evolution a massive white dwarf near the Chandrasekar limit is formed. We propose that the evolutionary sequence B is able to produce binary system with parameters similar to U Sco. Our best fitting model has initial parameters: $M_{sg,i} = 1.7 M_{\odot}$, $M_{wd,i} = 0.85 M_{\odot}$ and $P_i(RLOF) = 1.61 \text{ d}$. Based on evolutionary model we constructed a detailed theoretical model for U Sco. We found that the best fit parameters are: $M_{sg} = 0.94 M_{\odot}$, $M_{wd} = 1.31 M_{\odot}$, $\log L_{sg}/L_{\odot} = 0.42$, $\dot{M}_{sg} = 3.58 \times 10^{-8} M_{\odot} \text{ yr}^{-1}$ for $P_{orb} = 1.23056 \text{ d}$.

ACKNOWLEDGMENTS

This work is partly supported through grant 2-P03D-005-16 of the Polish National Committee for Scientific Research. JG and EE acknowledge support through Estonian SF grant 4338. EE acknowledges warm hospitality of the Astronomical Institute “Anton Pannekoek” where part of this work has been conducted. While in Netherlands, EE was supported by NWO Spinoza grant 08-0 to E. P. J. van den Heuvel.

REFERENCES

- Alexander D. R., Ferguson J. W., 1994, ApJ, 437, 879
- Anupama G. C., Dewangan G. C., 2000, AJ, 119, 1359
- Bahcall J. N., Pinsonneault M. H., 1992, Rev. Mod. Phys., 64, 885
- Bahcall J. N., Ulrich R. K., 1988, Rev. Mod. Phys., 60, 297
- Bahcall J. N., Pinsonneault M. H., Wasserburg G. J., 1995, Rev. Mod. Phys., 67, 781
- Barlow M. J. et al., 1981, MNRAS, 195, 61
- Caughlan G. R., Fowler W. A., Harris M. J., Zimmerman B. A., 1985, Atom. Data and Nucl. Data Tables, 32, 197
- Caughlan G. R., Fowler W. A., 1988, Atom. Data and Nucl. Data Tables, 40, 283
- Chanan G. A., Nelson J. E., Margon B., 1978, ApJ, 226, 963
- De Greve J.-P., 1993, A&ASS, 97, 527
- Eggleton P. P., 1983, ApJ, 268, 368

- Fowler W. A., Caughlan G. R., Zimmerman B. A., 1967, *ARA&A*, 5, 525
- Fowler W. A., Caughlan G. R., Zimmerman B. A., 1975, *ARA&A*, 13, 69
- Hachisu I., Kato M., Nomoto K., 1996, *ApJ*, 470, L97
- Hachisu I., Kato M., Nomoto K., Umeda H., 1999, *ApJ*, 519, 314
- Hachisu I., Kato M., Kato T., Matsumoto K., 2000, *ApJ*, 528, L97
- Harris M. J., Fowler W. A., Caughlan G. R., Zimmerman B. A., 1983, *ARA&A*, 21, 165
- Huebner W. F., Merts A. L., Magee N. H. Jr., Argo M. F., 1977, *Astrophys. Opacity Library*, Los Alamos Scientific Lab. Report No. LA-6760-M
- Iglesias C. A., Rogers F. J., 1996, *ApJ*, 464, 943
- Kahabka P., Hartmann H. W., Parmar A. N., Negueruela I., 1999, *A&A*, 347, L43
- Kato M., 1996, in: "Supersoft X-ray sources", ed. J. Greiner, *Lecture notes in physics*, vol. 472, Springer, p.15
- Kovetz A., Prialnik D., 1997, *ApJ*, 477, 356 (KP97)
- Kudryashov A. D., Ergma E. V., 1980, *Sov. Astron. Lett.*, 6, 375
- Li X.-D., van den Heuvel E. P. L., 1997, *A&A*, 322, L9
- Livio M., Pringle J. E., 1998, *ApJ*, 505, 339
- Livio M., Govarie A., Ritter H., 1991, *A&A*, 246, 84
- Marks P. B., Sarna M. J., Prialnik D., 1997, *MNRAS*, 290, 283
- Marks P. B., Sarna M. J., 1998, *MNRAS*, 301, 699 (MS98)
- Nomoto K., Nariai K., Sugimoto D., 1979, *PASP*, 31, 287
- Munari U., Zwitter T., Tomov T., Bonifacio P., Selvelli P., Tomasella L., Niedzielski A., Pearce A., 1999, *A&A*, 347, L39
- Paczyński B., 1967, *Acta Astron.*, 17, 287
- Paczyński B., 1970, *Acta Astron.*, 20, 47
- Pols O. R., Tout C. A., Eggleton P. P., Han Z., 1995, *MNRAS*, 274, 964
- Prialnik D., Livio M., 1995, *PASP*, 107, 1201
- Prialnik D., Kovetz A., 1995, *ApJ*, 445, 789 (PK95)
- Sarna M. J., De Greve J.-P., 1994, *A&A*, 281, 433
- Sarna M. J., De Greve J.-P., 1996, *QJRAS*, 37, 11
- Schaefer B.E., 1990, *ApJ*, 335, L39
- Schaefer B. E., Ringwald F. A., 1995, *ApJ*, 447, L45
- Schneider D. P., Greenstein J. L., 1979, *ApJ*, 233, 935
- Truran J. W., Livio M., Hayes J., Starrfield S., Sparks W. M., 1988, *ApJ*, 324, 345
- Verbunt F., 1993, *ARA&A*, 31, 93
- Warner B., 1995, *Cambridge Astrophysics Series*, No. 28, *Cataclysmic Variable Stars*, Cambridge Univ. Press, Cambridge
- Webbink R. F., Livio M., Truran J. W., Orio M., 1987, *ApJ*, 314, 653
- Williams G., 1983, *ApJS*, 53, 523
- Williams R. E., Sparks W. M., Gallagher J. S., Ney E. P., Starrfield S. G., Truran J. W., 1981, *ApJ*, 251, 221
- Ziółkowski J., 1985, *Acta Astron.*, 35, 199

